Optics Letters

Probing scattering resonances of Vogel's spirals with the Green's matrix spectral method

Aristi Christofi,[1] Felipe A. Pinheiro,[2] and Luca Dal Negro[1,3,*]

[1]Department of Electrical and Computer Engineering, Boston University, 8 Saint Mary's St., Boston, Massachusetts 02215, USA
[2]Instituto de Física, Universidade Federal do Rio de Janeiro, Rio de Janeiro-RJ, 21941-972, Brazil
[3]Division of Materials Science & Engineering, Boston University, 15 Saint Mary's St., Brookline, Massachusetts 02446, USA
*Corresponding author: dalnegro@bu.edu

Received 18 March 2016; accepted 24 March 2016; posted 28 March 2016 (Doc. ID 261505); published 20 April 2016

Using the rigorous Green's function spectral method, we systematically investigate the scattering resonances of different types of Vogel spiral arrays of point-like scatterers. By computing the distributions of eigenvalues of the Green's matrix and the corresponding eigenvectors, we obtain important physical information on the spatial nature of the optical modes, their lifetimes and spatial patterns, at small computational cost and for large-scale systems. Finally, we show that this method can be extended to the study of three-dimensional Vogel aperiodic metamaterials and aperiodic photonic structures that may exhibit a richer spectrum of localized resonances of direct relevance to the engineering of novel optical light sources and sensing devices.

OCIS codes: (290.5850) Scattering, particles; (290.4210) Multiple scattering; (350.4238) Nanophotonics and photonic crystals.

http://dx.doi.org/10.1364/OL.41.001933

The ability to efficiently design and characterize localized electromagnetic modes and photonic bandgaps in periodically ordered dielectric media unveiled fascinating analogies between electronic and classical wave phenomena that led to numerous device applications to optics and nanophotonics [1]. Optical metamaterials with periodically arranged resonant building-blocks of sub-wavelength dimensions have been recently demonstrated to exhibit unusual optical functionalities [2]. On the other hand, controlling light transport and optical resonances in disordered media with random refractive index fluctuations poses a significant challenge from a design perspective. Indeed, despite classical waves in random media sharing fundamental similarities with transport phenomena in electronic systems, such as the Anderson localization of light [3–5], disordered optical structures lack the reproducible and predictable behavior that is necessary for designing many advanced optical devices.

To circumvent these difficulties, artificial optical media with a tunable degree of aperiodic structural order generated by deterministic mathematical rules have emerged as an alternative platform for engineering novel devices [6–8]. Deterministic aperiodic structures manifest distinctive optical responses that cannot be found in either periodic or random systems, such as fractal transmission spectra and anomalous transport properties. Also, they have a rich spectrum of optical modes with various degrees of spatial localization, known as "critical modes." They manifest a power-law localization scaling with highly fragmented multi-fractal envelopes with applications in multi-mode lasing and optical sensing [8–13].

Among the various deterministic aperiodic optical systems investigated so far, the Vogel spiral arrays of nanoparticles are particularly appealing due to their wide structural tunability that interpolates in a tunable fashion in between short-range correlated amorphous/liquid systems and uncorrelated random ones [9–13]. Vogel spirals are ordered structures that lack both translational and rotational symmetry. Different from standard photonic crystals and quasi-crystals, their spatial Fourier spectra do not exhibit well-defined Bragg peaks, but rather, broad and diffuse circular rings whose position is controlled by simple design rules. The positions of particles in Vogel spiral arrays are simply obtained in polar coordinates by [14–16]

$$r = a\sqrt{n}, \tag{1}$$

$$\theta = n\alpha, \tag{2}$$

where $n = 0, 1, 2, \ldots$ is an integer, a is the scaling factor determining particle separation, and α is the divergence angle. In the case of the "sunflower spiral," also called the golden-angle spiral (GA-spiral), $\alpha \approx 137.508°$ is an irrational number. Previous studies have focused on the three most investigated types of aperiodic spirals, including the GA-spiral and two other Vogel spirals obtained by the following choice of divergence angles: 137.3° (i.e., α_1-spiral) and 137.6° (i.e., β_4-spiral). In order to efficiently design and engineer novel devices that fully leverage the critical modes of the photonic Vogel's spiral, we need to resort to a scalable approach capable of directly capturing the rich spectral-spatial properties of scattering resonances in open two-dimensional (2D) and three-dimensional (3D) large-scale aperiodic media.

In this Letter, we propose to address this important issue for both planar and 3D Vogel spiral metamaterials using the efficient Green's matrix method. The analysis of the Green's matrix spectra has been proven to be a very powerful tool to address

different aspects of light propagation in open random media, such as the Anderson localization of light [17–20] and matter waves [21], random lasing [22,23], light transport in nonlinear media [24], and superradiance in atomic random systems [25–28]. An analytical theory has been developed for the eigenvalue density of Green's matrices, providing fundamental insights into light propagation in disordered media [29–31]. However, the application of this powerful method has been mostly limited to random media so far. The purpose of the present Letter is, hence, to systematically apply this method to investigate multiple light scattering for Vogel spiral arrays, which will allow us to unveil the complex properties of their scattering resonances, which are not usually obtained by means of purely numerical methods, such as the finite difference time domain (FDTD) method.

To this end, we consider a system of N identical point-dipoles described by a scattering matrix $\mathbf{t}$ and arranged to form a Vogel spiral array subjected to an incident plane wave excitation Ψ_0. The Foldy–Lax self-consistent multiple scattering equations for the local excitation fields at the dipoles can be written as

$$\Psi(\mathbf{r}_i) = \Psi_0(\mathbf{r}_i) + \mathbf{t}\sum_{i,j=1}^{N} \mathbf{G}(\mathbf{r}_{ij})\Psi(\mathbf{r}_j), \tag{3}$$

where the complex-valued $3N \times 3N$ dyadic Green's matrix $\mathbf{G}(\omega, \mathbf{r}_{ij})$ describes the radiation scattered by the dipole located at $\mathbf{r}_j$ on the dipole located at $\mathbf{r}_i$ [17,20]. These equations can be derived directly from Maxwell's equations and treat multiple scattering exactly by taking all scattering orders into account [32]. The elements of the $3N \times 3N$ Green's matrix are equal to the Green's functions calculated from the relative positions $\mathbf{r}_{ij}$ of the N pointlike scatterers [33]:

$$\mathbf{G}_{ij}(\omega, \mathbf{r}_{ij}) = \begin{cases} -\frac{\exp(ikr_{ij})}{i4\pi r_{ij}}\left\{[\mathbf{U} - \hat{\mathbf{r}}_{ij}\hat{\mathbf{r}}_{ij}] - \left(\frac{1}{ikr_{ij}} + \frac{1}{(kr_{ij})^2}\right)[\mathbf{U} - 3\hat{\mathbf{r}}_{ij}\hat{\mathbf{r}}_{ij}]\right\} & \text{for } i \neq j, \\ 0 & \text{for } i = j, \end{cases} \tag{4}$$

where $\mathbf{U}$ is the unit matrix and k the wavenumber.

In this work, we will perform a direct numerical diagonalization of $\mathbf{G}$ and demonstrate that for strong scattering systems the eigenvalue spectra of Green's matrices are significantly different from the case of random systems, and that the corresponding eigenvectors closely reproduce the critically localized mode patterns of the Vogel spirals. Moreover, we determine the position and widths of the Vogel spiral resonances and correlate them with the spatial distribution of eigenmodes, showing that they group into different classes, in excellent agreement with prior work based on finite element simulations of dielectric nano-cylinders of finite size [12]. Finally, we fully leverage the scalability of the efficient Green's matrix approach by considering a 3D Vogel metamaterial structure, obtained by superimposing planar Vogel spiral layers, and computing the distribution of its scattering resonances as well as the spatial distribution of its most localized one.

In Fig. 1 we show the computed distribution of eigenvalues of the Green's matrix for a 2D GA-spiral with 300 identical scatterers for different values of kl; the bare Ioffe–Regel parameter kl (where l is the mean free path) that measures the disorder strength. We assume a Breit–Wigner model for the scatterers with one sharp resonance of width Γ_0 at the frequency position ω_0. The incident frequency is set to be the resonant frequency ω_0 for which the scattering cross-section of the dipoles is maximal [33]. We found that for weak scattering systems ($kl \approx 100$) this distribution is qualitatively very similar to the one reported for random scatterers, featuring a disk-like eigenvalue distribution in agreement with the analytical random matrix theory [30]. On the other hand, we found that for smaller values of kl (i.e., increased scattering) the distribution of eigenvalues significantly deviates from the case of disordered systems. In particular, as shown in panels (a)–(d) of Fig. 1 for the representative case of the GA-spiral, by reducing the kl values, the eigenvalues cluster around an increasing number of spiral branches. For small systems, the presence of hyperbolic branches in the eigenvalue distribution of the Green's matrix of random systems was previously reported and attributed to the onset of proximity scattering effects induced by short-range scattering correlations [17]. We believe that the distinctively different shapes and the larger number of branches demonstrated for the Vogel spirals directly reflect the increased degree of spatial correlations for these systems compared to random ones. Additionally, as clear from Fig. 1(d), the eigenvalues of the Vogel spirals cluster around the line $\mathrm{Re}\,\lambda = -1$. We recall here that the real and imaginary parts of the eigenvalues of the $\mathbf{G}$ matrix are associated to the relative widths $(\Gamma - \Gamma_0)/\Gamma_0$ and frequency positions $(\omega - \omega_0)/\Gamma_0$ of the scattering resonances [17], and that the following relations approximately hold: $\mathrm{Re}\,\lambda(\omega_0) \simeq (\Gamma - \Gamma_0)/\Gamma_0$ and $\mathrm{Im}\,\lambda(\omega_0) \simeq (\omega - \omega_0)/\Gamma_0$. Therefore, since the real part of the eigenvalues is related to the decay rate of the modes, a clustering of eigenvalues around the line $\mathrm{Re}\,\lambda = -1$, as in Fig. 1(d), evidences the formation of long-lived modes in this region.

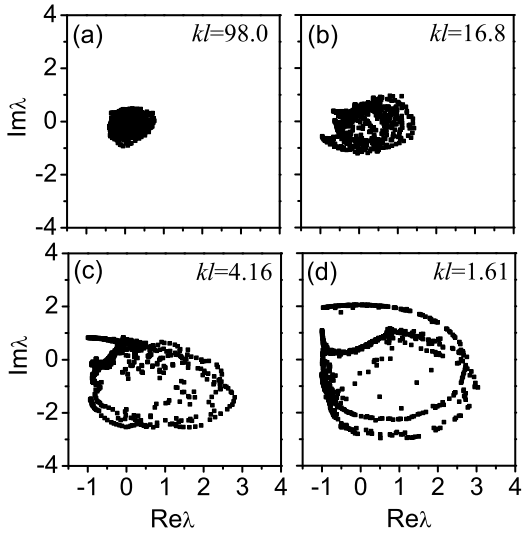

Fig. 1. Representative Green's matrix eigenvalues distribution for a 2D GA-spiral array consisting of 300 scattering particles for different values of kl.

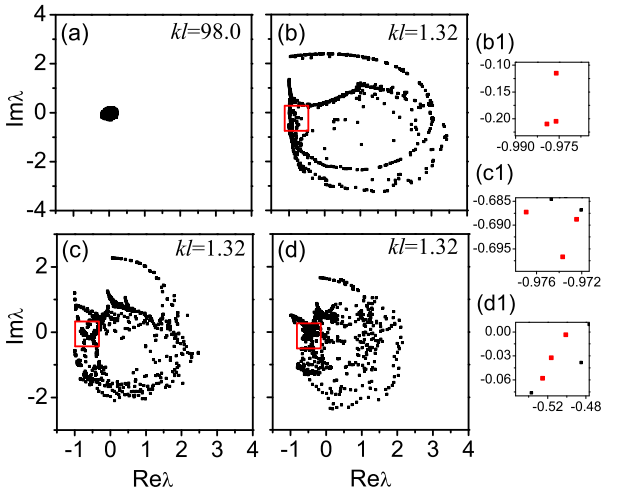

Fig. 2. (a) A representative Green's matrix eigenvalues distribution for large kl values of a 2D α_1-spiral array. (b)–(d) The eigenvalues distributions for GA-, α_1-, and β_4-spiral arrays, respectively, for the kl value of interest. The regions of interesting eigenmodes, close to the origin, are marked with red squares. All the 2D Vogel spiral arrays consist of 300 scattering particles. In the margin, we show three panels (b1), (c1), and (d1) where we zoom into the specific eigenvalues of interesting modes, from the eigenvalues distribution of the diagrams (b), (c), and (d), respectively.

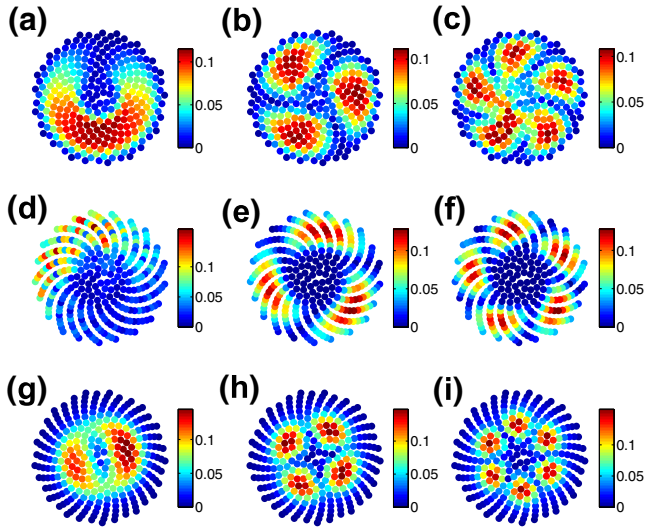

Fig. 3. Distribution of the electric field magnitude of 300 scattering particles, of (a)–(c) class C in a GA-spiral, (d)–(f) class B in an α_1-spiral, and (g)–(i) class D in a β_4-spiral. The real and imaginary parts of the 9 eigenvalues with the corresponding (a)–(i) modes are: (−0.979, −0.210), (−0.976, −0.205), (−0.976, −0.115), (−0.974, −0.697), (−0.972, −0.689), (−0.977, −0.687), (−0.525, −0.058), (−0.516, −0.032), and (−0.501, −0.004), respectively. The eigenvalues are shown in the panels of the margin of Fig. 2.

A similar behavior was also observed for the α_1 and β_4 Vogel spiral geometries.

Figure 2 summarizes our findings, also, for the α_1 and β_4 Vogel spirals. We notice that for the large kl values (i.e., weak scattering), we always observe a disk-like eigenvalue distribution independently of the specific spiral geometry. In Figs. 2(b)–2(d), we report representative results for all of the investigated spiral geometries in the strong scattering limit. The red squares indicate the regions of the eigenvalue distributions where the longest-lived modes were found. There are also regions of eigenvalues, away from the origin with a larger real part, that correspond to leaky modes and isolated clusters of eigenvalues that correspond to degenerated modes. Here it is important to emphasize that the Green's matrix spectral method provides important physical information about light transport in open media that cannot be obtained via other numerical methods, such as FDTD. Indeed, in contrast to FDTD, the Green's matrix spectral method allows one to not only obtain the frequency positions and lifetimes (the inverse of the resonance width) of scattering resonances, but also to correlate them to the spatial distribution of optical quasi-modes, as it will be discussed in the following. Hence, this method permits access to the full spectral information on Vogel spiral arrays, which have never been probed so far, as previous studies have been based on purely numerical results [12,13].

The spatial distributions of the long-lived modes of Vogel spirals can be obtained by studying the eigenvectors of the corresponding Green's matrix, as shown in Fig. 3. Using the spectral Green's matrix method, we can conveniently identify different classes of modes by seeking eigenvalues with small real parts and by moving vertically in the eigenvalue distribution diagram (Fig. 2) in order to scan the mode frequency. By performing this procedure, we have been able to reliably identify all of the classes of the Vogel spiral modes previously reported [12,13] and extract quantitative information on the localization character of each of these modes, in addition to their position in frequency and widths. These classes of modes, which are located at the multi-fractal photonic band-edges of the dielectric Vogel spiral arrays, have a quality factor Q that scales linearly with frequency [12,13]. As an example, in Fig. 3 we plot the distribution of the electric field magnitude of the GA-spiral (a)–(c), α_1-spiral (d)–(f), and β_4-spiral (g)–(i), with 300 scattering particles. By referring to the mode classification in [12,13], we can see that for the GA-spiral the Green's matrix approach correctly yields the modes of class C. For the α_1-spiral, we obtain the modes of class B while our procedure demonstrates for the first time that the modes of class D can also be supported by the β_4-spiral geometry. We notice that the modes in this class have been reported only for the GA-spiral before [13]. The modes of class C are located near the boundary of the spiral structure, and therefore, exhibit stronger radiation leakage while the modes of class B and of class D, being mostly localized closer to the center of the spirals, have a smaller radioactive character.

The superior scalability of the proposed design strategy allows for a novel approach to engineer 3D aperiodic photonic structures and metamaterials. Indeed, this method can be applied to conceive a 3D Vogel spiral metamaterial as schematized in Fig. 4(a). The structure under consideration is a 3D GA-spiral formed by vertically cascading seven layers each of 300 scatterers in each layer. A similar study of the Green's matrix eigenvalues distributions is carried out for this 3D metamaterial, and the results for the two representative distributions at different kl values are shown in Fig. 4(b). In the weak scattering limit ($kl \approx 98$), we observe an eigenvalue

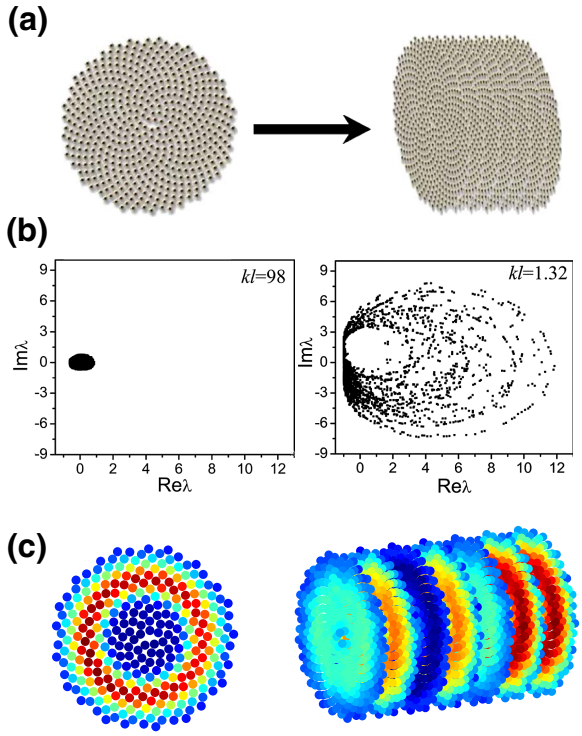

Fig. 4. (a) From a 2D Vogel spiral array to a 3D Vogel spiral metamaterial, consisting of 7 layers of 300 scattering particles each. (b) Two representative Green's matrix eigenvalues distributions for two different values of kl for a 3D GA-spiral metamaterial consisting of 7 layers with 300 scattering particles in each layer. (c) A characteristic long-lived mode of a 2D GA-spiral array (left-hand diagram) and a selected mode of the 3D GA-spiral metamaterial (right-hand diagram). The real and imaginary parts of the 2 eigenvalues with the corresponding modes are (−0.802, −0.226) (left-hand diagram) and (−0.980, −0.680) (right-hand diagram).

distribution that is very similar to the case of random systems. On the other hand, in the strongly scattering case ($kl = 1.32$), we demonstrate the formation of several spiral branches and observe again the clustering of eigenvalues around the line $\mathrm{Re}\,\lambda = -1$. We conclude that, despite the difference in dimensionality and particle numbers, 3D Vogel spiral arrays exhibit qualitatively similar modal properties with respect to their 2D counterparts. To conclude our study, in Fig. 4(c) we compare the spatial distribution of a radially localized scattering resonance of a representative 2D GA-spiral array [with the eigenvalue inside the red square of the distribution of Fig. 2(b)] with the one of the corresponding 3D structures computed from the same region of the eigenvalues distribution map. We notice that the two modes display remarkable structural similarities, revealing their common nature. Based on the proposed Green's matrix approach, future work will address the design of localized optical resonances in 3D aperiodic media.

In summary, we applied the rigorous Green's matrix method to the analysis of the scattering resonances of Vogel spiral arrays and demonstrated that the eigenvalues and eigenvectors distribution of the Green's matrix allow us to obtain important physical information on the spatial nature of the modes, their lifetimes and their classification type, at a small computational cost and for large-scale systems. We have also shown that this method can be extended to the study of 3D Vogel aperiodic metamaterials and aperiodic photonic structures that may exhibit an even richer spectrum of long-lived modes of direct relevance to novel optical light sources and sensing devices.

Funding. U.S. Army Research Laboratory (ARL) (W911NF-12-2-0023); Coordenação de Aperfeiçoamento de Pessoal de Nível Superior (CAPES) (BEX 1497/14-6); Conselho Nacional de Desenvolvimento Científico e Tecnológico (CNPq) (303286/2013-0).

Acknowledgment. F. A. P. thanks the hospitality of the Optoelectronics Research Centre and Centre for Photonic Metamaterials, University of Southampton, where part of this work was done.

REFERENCES

1. J. D. Joannopoulos, S. G. Johnson, J. N. Winn, and R. D. Meade, *Photonic Crystals: Molding the Flow of Light*, 2nd ed. (Princeton University, 2008).
2. N. Engheta and R. W. Ziolkowski, *Metamaterials: Physics and Engineering Explorations* (IEEE/Wiley, 2006).
3. P. W. Anderson, Phys. Rev. **109**, 1492 (1958).
4. A. Lagendijk, B. A. van Tiggelen, and D. S. Wiersma, Phys. Today **62** (8), 24 (2009).
5. S. E. Skipetrov and J. H. Page, New J. Phys. **18**, 021001 (2016).
6. E. Macia, Rep. Prog. Phys. **75**, 036502 (2012).
7. L. Dal Negro and S. V. Boriskina, Laser Photon. Rev. **6**, 178 (2012).
8. L. Dal Negro, *Optics of Aperiodic Structures: Fundamentals and Device Applications* (Pan Stanford, 2014).
9. J. Trevino, H. Cao, and L. Dal Negro, Nano Lett. **11**, 2008 (2011).
10. L. Dal Negro, N. Lawrence, and J. Trevino, Opt. Express **20**, 18209 (2012).
11. N. Lawrence, J. Trevino, and L. Dal Negro, Opt. Lett. **37**, 5076 (2012).
12. J. Trevino, S. F. Liew, H. Noh, H. Cao, and L. Dal Negro, Opt. Express **20**, 3015 (2012).
13. S. F. Liew, H. Noh, J. Trevino, L. Dal Negro, and H. Cao, Opt. Express **19**, 23631 (2011).
14. J. A. Adam, *A Mathematical Nature Walk* (Princeton University, 2009).
15. E. Macia, *Aperiodic Structures in Condensed Matter: Fundamentals and Applications* (CRC Press/Taylor & Francis, 2009).
16. G. J. Mitchison, Science **196**, 270 (1977).
17. M. Rusek, J. Mostowski, and A. Orlowski, Phys. Rev. A **61**, 022704 (2000).
18. S. E. Skipetrov and I. M. Sokolov, Phys. Rev. Lett. **112**, 023905 (2014).
19. C. E. Maximo, N. Piovella, Ph. W. Courteille, R. Kaiser, and R. Bachelard, Phys. Rev. A **92**, 062702 (2015).
20. F. A. Pinheiro, M. Rusek, A. Orlowski, and B. A. van Tiggelen, Phys. Rev. E **69**, 026605 (2004).
21. P. Massignan and Y. Castin, Phys. Rev. A **74**, 013616 (2006).
22. F. A. Pinheiro and L. C. Sampaio, Phys. Rev. A **73**, 013826 (2006).
23. F. A. Pinheiro, Phys. Rev. A **78**, 023812 (2008).
24. B. Gremaud and T. Wellens, Phys. Rev. Lett. **104**, 133901 (2010).
25. E. Akkermans, A. Gero, and R. Kaiser, Phys. Rev. Lett. **101**, 103602 (2008).
26. A. A. Svidzinsky, J. T. Chang, and M. O. Scully, Phys. Rev. A **81**, 053821 (2010).
27. L. Bellando, A. Gero, E. Akkermans, and R. Kaiser, Phys. Rev. A **90**, 063822 (2014).
28. S. E. Skipetrov and I. M. Sokolov, Phys. Rev. Lett. **114**, 053902 (2015).
29. A. Goetschy and S. E. Skipetrov, Europhys. Lett. **96**, 34005 (2011).
30. A. Goetschy and S. E. Skipetrov, Phys. Rev. E **84**, 011150 (2011).
31. S. E. Skipetrov and A. Goetschy, J. Phys. A **44**, 065102 (2011).
32. L. Tsang, J. A. Kong, K. Ding, and C. O. Ao, *Scattering of Electromagnetic Waves: Numerical Simulations* (Wiley, 2001).
33. A. Lagendijk and B. A. van Tiggelen, Phys. Rep. **270**, 143 (1996).